Design and Deployment of Dual MooSci Lunar Scintillometers at Las Campanas Observatory

K.W. Cook, S. Villanueva Jr., D.L. DePoy, J.L. Marshall, J.P. Rheault, R.D. Allen, and D.W. Carona

Department of Physics and Astronomy, Texas A&M University, 4242 TAMU, College Station, TX 77843-4242, USA

J.E. Thomas-Osip[1], G. Prieto[1], A. Berdja

The Giant Magellan Telescope Organization (GMTO), P.O. Box 933, Pasadena, CA 91109-0933, USA

ABSTRACT

Lunar scintillometers provide information about atmospheric conditions at astronomical observing sites. In particular, they are able to measure the ground layer turbulence and its effect on astronomical seeing. In this paper we describe a new lunar scintillometer, MooSci, to aid in the site characterization campaign for the Giant Magellan Telescope (GMT). MooSci has been tested and confirmed to provide reliable data for the reconstruction of turbulence profiles. In this paper the instrument design and testing is described.

1. Introduction

Motion of light as it moves through turbulence in Earth's atmosphere, or "seeing", has long been a concern of ground-based observatories by placing a limit on the achievable angular resolution of a facility. Today, adaptive optics (AO) help make it possible for ground-based observatories to achieve a resolution that surpasses that of some space-based missions. Roddier (1981) provides a detailed summary of our knowledge linking atmospheric turbulence to scintillation. By measuring the scintillation at a site the turbulence profile of the atmosphere can be reconstructed. This will help existing observatories to develop better AO systems and identify if a particular site is optimal for planned next generation telescopes. Several instruments capable of measuring this scintillation have been created.

Devices that measure the scintillation of astronomical objects, called scintillometers, have been designed and deployed that target a variety of astronomical objects. Scidar (Vernin & Muñoz-Tuñón

[1]Las Campanas Observatory, Casilla 601, Colina El Pino, La Serena, Chile

1992) uses double star systems to measure the turbulence at a site, while the MASS is a single star scintillometer (Tokovinin 2007). Others have proposed and designed a solar scintillometer (Beckers et al. 1997). Lunar scintillometers have also been used (Hickson & Lanzetta 2004) (Rajagopal et al. 2008) (Tokovinin et al. 2010) as an effective measure of scintillation. Stellar scintillometers are in use at many observatories and monitor nighttime conditions year long. Stellar scintillometers, like the MASS, are most useful for the reconstruction of the turbulence profile of the upper atmosphere, where stellar scintillation is strongest. The disk of extended objects results in scintillation that averages out in the upper layers while the lowest layers remain relatively strong. Extended objects are therefore most effective for reconstruction of the ground layer atmospheric turbulence, the region most important to understand when considering observatory design and its location on a particular peak. (Tokovinin 2007).

The Sun, planets, and the Moon are possible potential extended target objects. Planets are not the best choice largely due to the low signal received from them. The Sun provides plenty of signal and is observable year round; however, daytime conditions can differ from those during the night. The best target for characterizing night time conditions in low levels of the atmosphere above a telescope site is the Moon, which provides adequate signal and is observable during the night. The Moon presents its own challenges, such as its phases and being observable for only a portion of the month. The phases lower the signal received and can lead to a signal to noise ratio (S/N) lower than that needed in a lunar scintillometer. This limits the amount of time in a month that the Moon can be observed.

In this paper we present a new lunar scintillometer, called MooSci (Villanueva et al. 2010). In §2 we provide a review of the relevant ideas in the physics of scintillation. The MooSci design is explained in §3, including the mechanical and electrical details along with a description of the data acquisition system. Laboratory Testing will be discussed in §4. Finally, in §5 the results from the deployment and initial observations from the first two MooSci units at the future site of the Giant Magellan Telescope (GMT) at Las Campanas Observatory (LCO) are discussed.

2. Scintillation Physics

Roddier (1981) gives a detailed discussion of the current knowledge of scintillation and how it is caused by atmospheric turbulence. Here we provide a basic overview of the relevant scintillation physics and refer to Roddier (1981) for a comprehensive review. Light bends due to changes in the refractive index of a medium at an interface. The refraction is dependent on a variety of factors such as temperature, density, and pressure. Prior to interacting with the Earth's atmosphere, light is in an environment where the values of these factors are very low. As it approaches the surface of the Earth, it passes through interfaces at atmospheric layers in which these and other factors can change. At each interface, or atmospheric layer, the light is bent and produces the familiar "twinkling" of the stars, or scintillation. The effect is that the shape of a flat wavefront becomes distorted as it passes through atmospheric layers. These distortions act as a series of weak positive

and negative lenses. Positive lenses result in a higher intensity measured from the ground while negative lenses decrease the measured intensity.

These lenses or distortions occur at multiple layers in the atmosphere and work together to disturb the wavefront. For Kolmogorov turbulence, the most commonly used model of a chaotic turbulent field, the structure function, $D_n(d)$, measures the variation in the index of refraction between two points in the atmosphere with a displacement, d:

$$D_n(d) = C_n^2(z)d^{2/3} \tag{1}$$

The structure function constant, $C_n^2(z)$, is a function of height, z, of the different atmospheric layers and is a scaling factor. It provides a measure of the strength of the turbulence. A higher value indicates a larger variation in the index of refraction between these points and thus a more turbulent atmosphere and greater scintillation.

Hickson & Lanzetta (2004) present a design for a scintillometer that uses detectors placed along a linear array. In this design each detector is baffled so that it may only see a cone of light extending above it. The angular size of the cone is defined by the aperture placed in front of the detector. Two detector's light cones overlap at a specific height above the ground that is determined by their separation. In the overlap region, common scintillation is detected by both detectors and can later be extracted from the data as a covariance signal. Detectors of a larger separation can probe higher into the atmosphere. By creating an array, one can achieve peak sensitivities at different levels of the atmosphere for each baseline, thereby recreating the atmospheric turbulence. Rajagopal et al. (2008) also use this type of configuration in the design of LuSci. They also provide the relation needed to extract the covariance, $C_I(r)$, between two detectors that are spaced a distance, r, apart:

$$C_I(r) = \int_0^\infty W(r,z)C_n^2(z)\ dz \tag{2}$$

where z is the line of sight height above the detectors, W(r,z) is a weighting function, and $C_n^2(z)$ is the structure function constant seen in Equation 1. The weighting function takes into account many factors including wind speed, the shape of the Moon based on its phase, apparent diameter of the Moon, and the angle of the Moon's terminator with respect to the detector baseline. Each baseline is sensitive to a range of heights with its peak sensitivity being higher as r increases, as shown in Figure 1, which shows individual baselines as well as the sensitivity of a single detector.

The C_n^2 value of each baseline, which relates to the strength of the atmospheric turbulence, is calculated based on the measured covariances. With multiple baselines probing successively higher into the atmosphere, this method determines where most of the scintillation originates. Different sites may have different $C_n^2(z)$ values. This allows a lunar scintillometer to be useful for site selection of next generation telescopes, and in understanding the details of the atmosphere at a particular site. This can inform smarter telescope facility construction and AO systems.

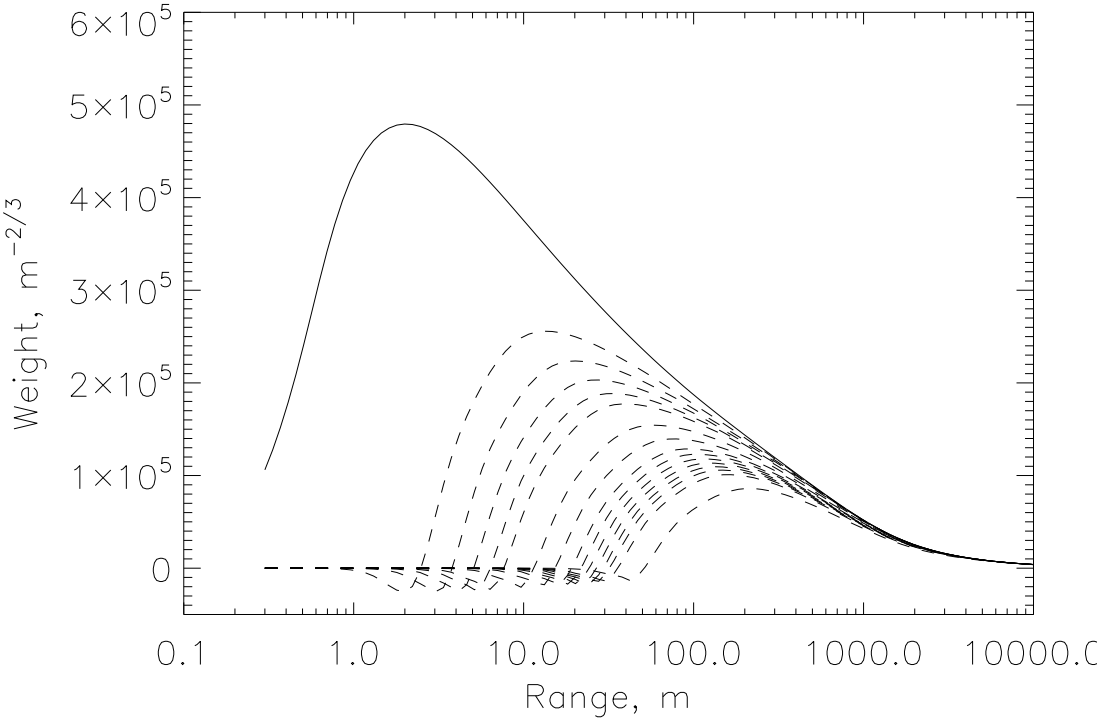

Fig. 1.— An example of the weighting function as calculated for the Full Moon of March 2011. The solid line is for a single detector. The dashed lines are individual baselines within the array. The curves with the shortest baselines peak on the left and increase in length to the right. The largest baselines have peak sensitivities at the greatest heights.

From a covariance signal the structure function constant can be extracted using Equation 2. By measuring C_n^2 over the entire atmosphere, or at least over the region of interest, the Fried parameter can be calculated for that region:

$$r_0 = [16.699\lambda^{-2} \sec\gamma \int_0^\infty C_n^2(z)\ dz]^{3/5} \tag{3}$$

where λ is the wavelength and γ is the zenith angle of the Moon at the time of observation. The Fried parameter defines the average size of the perturbative cell that the light passes through. It is also inversely proportional to the seeing,

$$\alpha_{seeing} \propto \frac{\lambda}{r_0} \tag{4}$$

3. MooSci Design and Operations

3.1. Mechanical Design

MooSci uses the basic design of Hickson & Lanzetta (2004) and Rajagopal et al. (2008), and uses a linear array of photodiodes to measure brightness fluctuations of the Moon. Correlations in the signal detected in the overlap region of two detectors can be extracted as covariance data. Two MooSci units have been produced and have been used for site characterization on the future site of the GMT at Las Campanas Observatory. MooSci uses many of the design elements present in LuSci (Tokovinin et al. 2010) and seeks to be an improvement over that design. The MooSci detectors have the same linear spacing as LuSci but are symmetric about the central detector, giving MooSci twice the total length. The location of each detector is at 0, 12, 15, 17, 21, 40, 59, 63, 65, 68, and 80 cm, and are shown in Figure 2. These baselines allow for atmospheric probes as low as 10m and ranging as high as 500m when the instrument is used as a single array. MooSci can also be used as two independent arrays due to the symmetry in the the detectors about the central position. In this configuration MooSci does not measure scintillation as high into the atmosphere but provides a detailed check on its own capabilities.

The MooSci design includes 11 photodiode modules, the beam forming the baseline, two electrical busses, the main electronics box, a dovetail plate which connects the other hardware pieces to the mount, and the mount itself. These are shown in Figure 3 as well as auxiliary components including a webcam, finder scope, and declination counterweight.

The 11 photodiode modules are responsible for signal detection and initial processing before the signal is sent to the main electronics box. The electronics of these modules will be discussed in the next section. Since the MooSci design uses no lenses or mirrors, the field of view is set by the mechanical design of the modules. Each module is a light-tight aluminum box or "can" containing a photodiode placed below a 50.8mm length 12.7mm diameter optical tube. A sapphire window

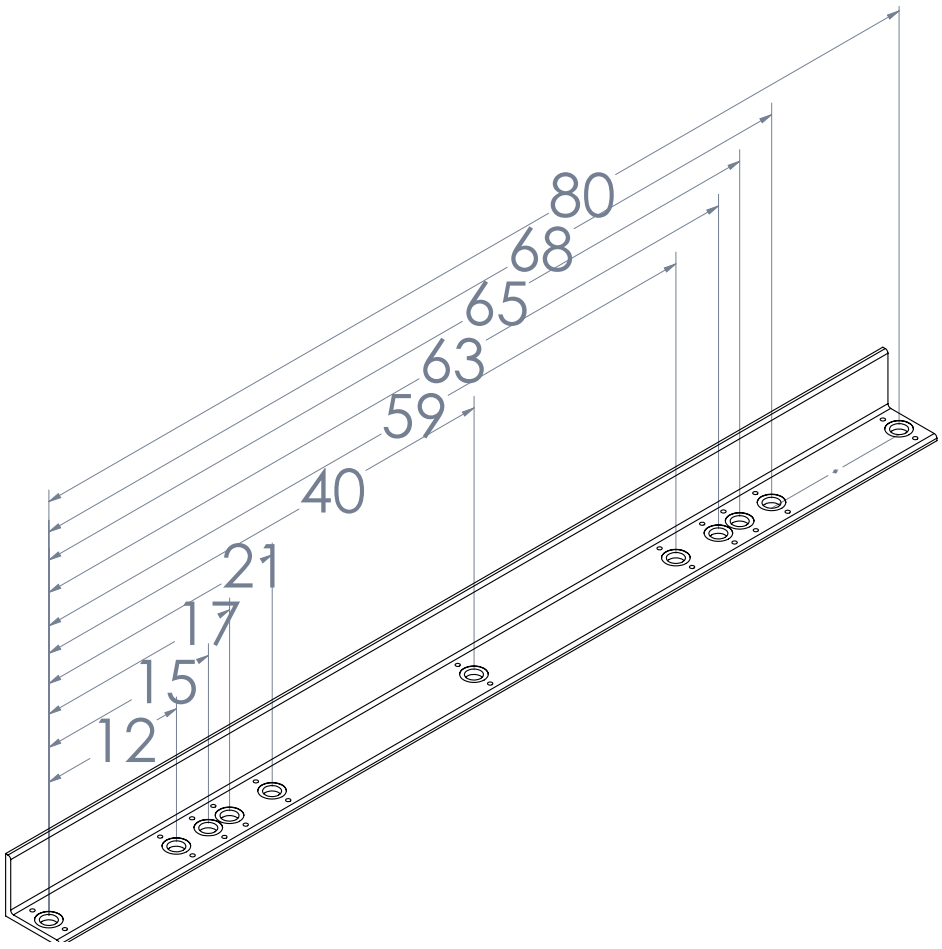

Fig. 2.— Mechanical drawing of the MooSci main baseline with detector spacings labeled. The shortest baseline is 2cm and the longest uses the entire array and is 80cm. Spacings are given in centimeters.

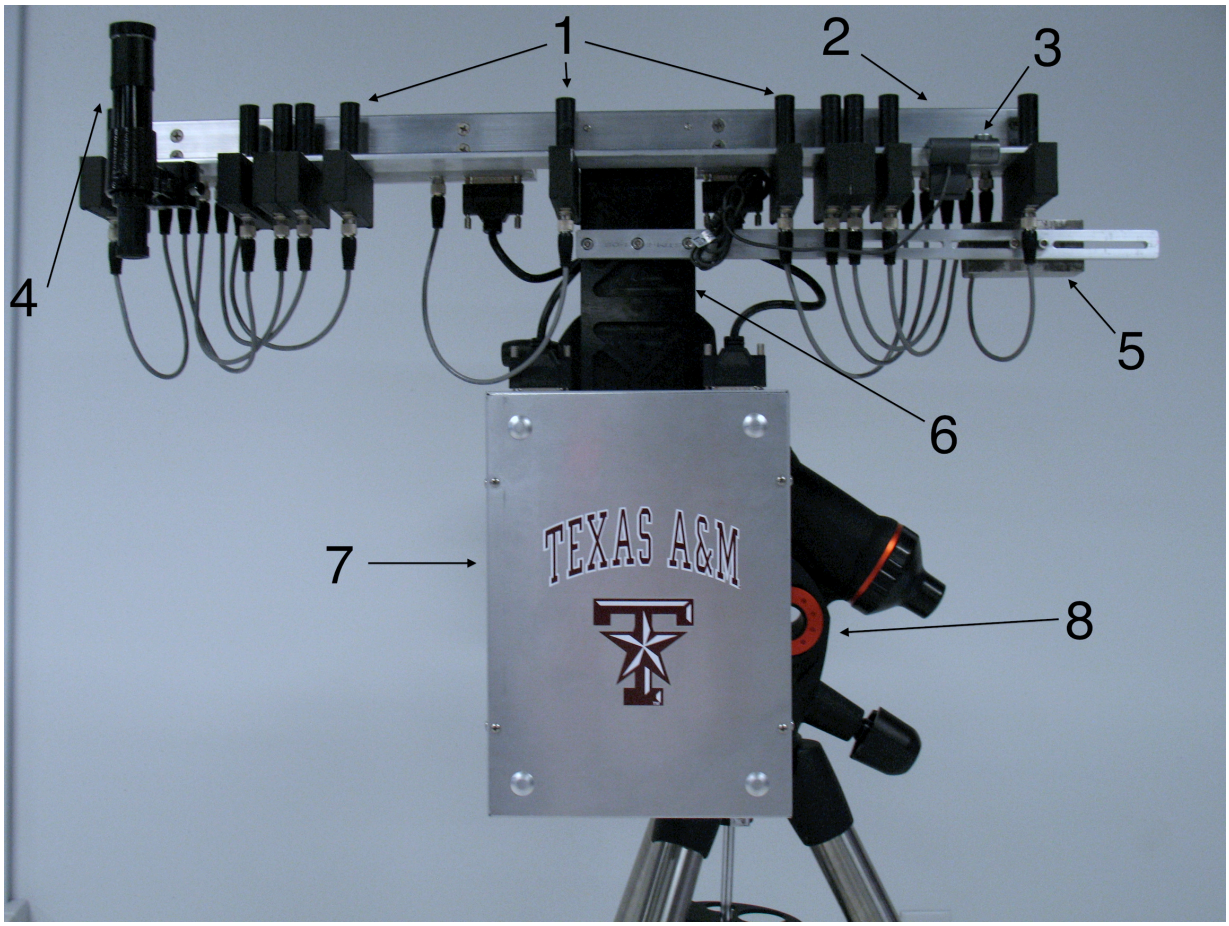

Fig. 3.— Image of the MooSci design with components labeled. The labels point to the components: (1) the individual photodiode modules, (2) the array beam, (3) the webcam, (4) the finder scope, (5) a declination counterweight, (6) the dovetail plate, (7) the main electronics box, and (8) the mount.

is placed inside of the optical tube to protect the photodiode. The second MooSci, MooTwo, has a slightly higher sensitivity than the original instrument; this resulted in the instrument just saturating on the Full Moon. The sapphire windows were replaced with a 0.1 neutral density filter. This change brought the signal down to the level of the first unit and still provides protection to the photodiode. The photodiode is placed 16mm below the optical tube giving each module a field of view of 6° on the sky. This field of view also sets the requirement that the mount be able to track within ±3° of the Moon.

MooSci includes increased baffling in both RA and Dec as compared to LuSci. This allows MooSci to cut out more background noise from the sky but increases the accuracy with which the instrument must be able to point and track. This is easily achieved with most advanced amateur computer controlled mounts.

3.2. Electrical Design

This section will discuss the details of the electrical design; discussion of the tests conducted with the instrument are deferred to §4. A high signal-to-noise (S/N) ratio of 10^4 at 100Hz is required because the fluctuations of the Moon's signal occur at 1 in 10^{-4} at that frequency (Villanueva et al. 2010). The MooSci electronics provide low noise in order to reach the required S/N. Figure 4 shows the inside of one of the photodiode modules with the printed circuit board (PCB) and electronics. The Hamamatsu S2387-66R photodiode is centered underneath the optical tubes and detects the photons which are then converted to a voltage signal. Preprocessing is done by the remaining electronics in the board. The electrical schematic is shown in Figure 5. The LuSci instrument (Tokovinin et al. 2010) separates the AC from the DC signal. Any AC signal greater than 0.1Hz is amplified and signal below this value is lost. The DC signal is monitored separately to identify any anomalies in the data. With MooSci the electronics are designed so that no low frequency signal will be lost. MooSci amplifies all of the collected signal and then applies a constant offset. The offset centers the zeropoint at a -10VDC output from the 16-bit Analog-Digital Converter (ADC). This allows MooSci to filter only the high bandpass signal that contains no scintillation data without cuts to the low frequencies where scintillation data may exist. This also guarantees that there is no electronic phase shift between signals. Two feedback loops filter out signals greater than 800Hz where no scintillation data is expected. After processing and amplification the signal is sent out of the can via a 4-pin connector. The offset places the signal range between ±10VDC to fit within the acceptable range of the ADC data acquisition device in the main electronics box. This electronic configuration is repeated inside each of the 11 photodiode modules.

Another improvement in the MooSci design is greatly reduced optical and electronic crosstalk between the individual detectors. This was accomplished by mounting each channel in its own can, strongly limiting the light each detector can see to its individual light cone and eliminating reflections or other unwanted light. The cans also provide a Faraday cage for each PCB board separately, reducing the possibility of electrical crosstalk.

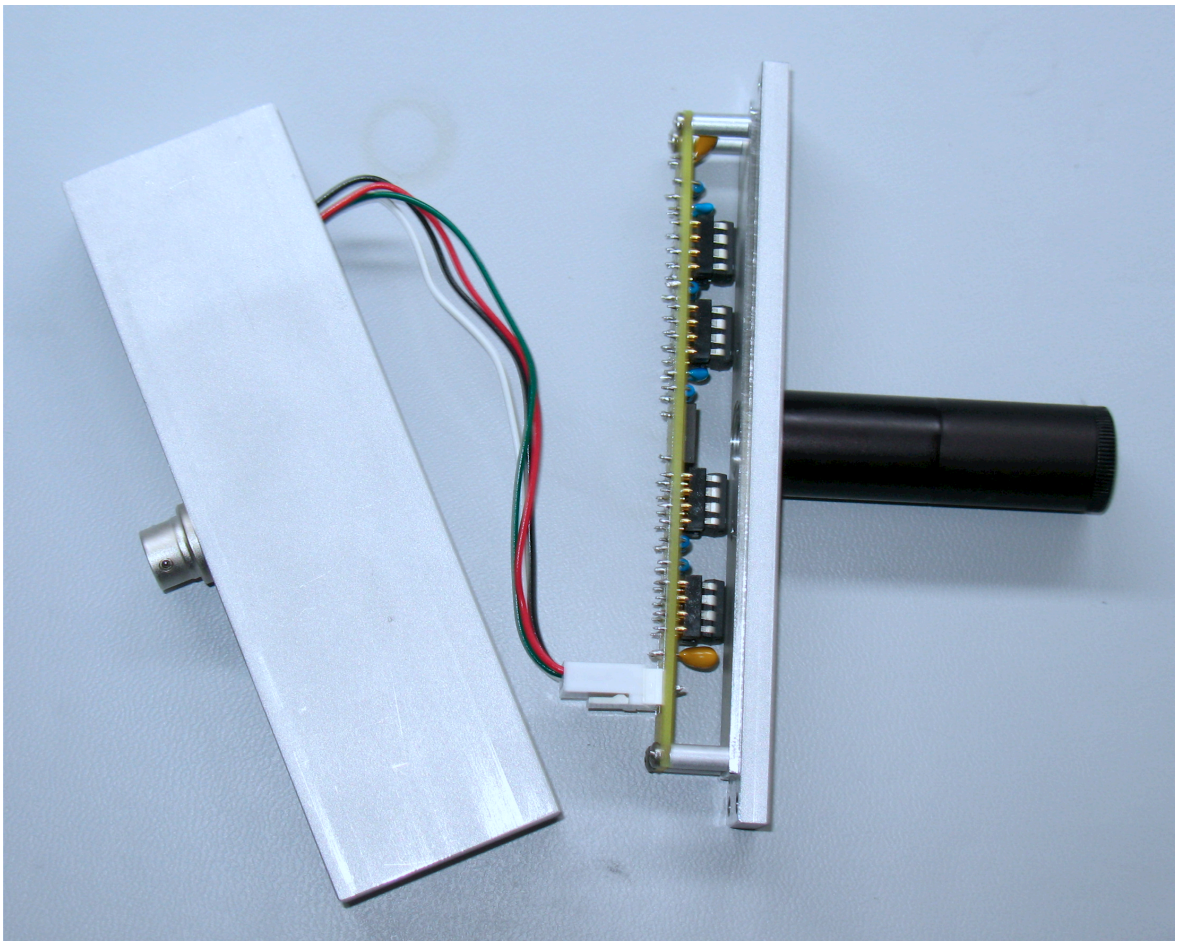

Fig. 4.— The inside of one of the photodiode modules. The photodiode sits directly beneath the optical tubes, collecting and then relaying the signal to the other components in the board. After this preprocessing the signal is sent out of the module via the 4-pin connector.

Once the signal leaves the modules it is sent via shielded cables to one of the two electrical busses and on to the main electronics box. Here all data is collected by the Measurement Computing USB-1616FS 16-bit ADC data acquisition device and sent outside of the instrument via USB cable. The entire instrument is powered by a ±15VDC power supply.

3.3. Data Acquisition

MooSci can be operated remotely each month within ±6 days of the Full Moon via a laptop which can be accessed using a Virtual Network Computing (VNC) connection. The laptop runs the instrument control software which is programmed with National Instruments LabVIEW language. This software displays a running 1 minute time averaged power spectrum of any two consecutive channels. A sudden change in the profile of the power spectrum can indicate a problem in the data and can be monitored by the user. A webcam aligned with MooSci's optical axis also provides visual feedback on tracking, pointing, and sky conditions to the user. Clouds, for instance, will be seen in the signal and the power spectrum. In this event the webcam allows the user to confirm the presence of the clouds and determine when the sky becomes clear and observations can be resumed.

At the beginning of an observing night a measurement is made with the optical tubes of the photodiode modules blocked off. These dark frames have a signal of ∼-9VDC and provide a measurement of the "baseline signal" as measured at the Texas A&M Physics Observatory. Increases in this value or differences between modules are an indication of problems with the unit. Observations are also taken with the modules open to light but pointed toward a dark area on the sky. These measurements are the total noise in the observations including both sky background and instrumental noise. These measurements also provide the total noise used in determining the S/N. The sky frames are taken 2-3 times during the course of the night to account for the change in the sky signal while the Moon is transiting vs when the Moon is near the horizon. MooSci is then pointed at the Moon to obtain scintillation data. The instrument and ADC collect data identically when taking dark, sky, and Moon data; a tag is placed in each filename by the software to easily identify the data type at a later date. Data can also be collected without saving if troubleshooting is needed.

Another noise reduction technique employed is using a high sampling rate. Data is collected by the ADC at a rate of 10kHz. This rate is faster than the response time of the photodiodes but allows for averaging of the signal. Generally, data are averaged to an effective sampling rate of 500Hz which provides a $\sqrt{20}$ lower effective electrical noise.

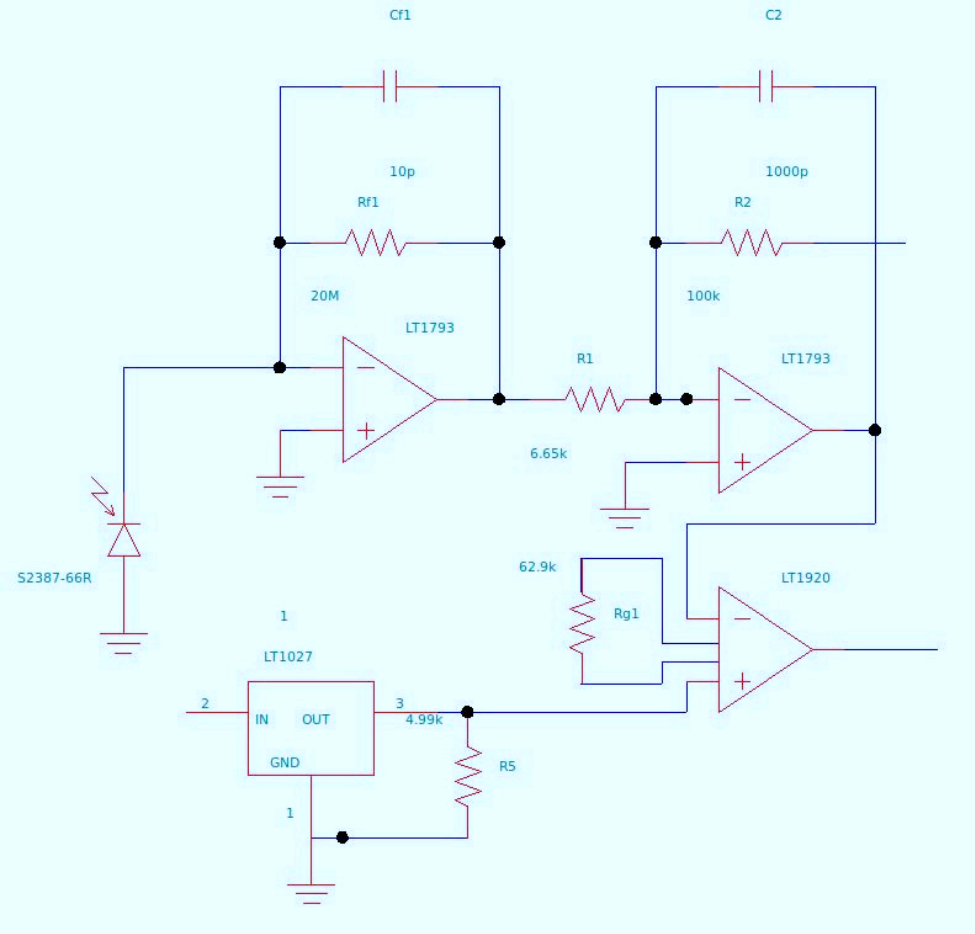

Fig. 5.— The electrical schematic for MooSci. After collection by the photodiode the signal is filtered, amplified, and inverted in the two LT1793 op amps. The LT1027 voltage regulator supplies a 5VDC offset to the LT1920 instrumentation amplifier which compares this with the signal from the second LT1793 and outputs the result.

4. MooSci Testing

4.1. Signal to Noise Analysis

Lunar scintillation is a subtle effect with fluctuations generally occurring at 1 part in 10^{-4} at 100Hz. MooSci is therefore required to make detections with a S/N of 10^4. The S/N is not constant over a lunation or over a single night. Over multiple days the signal level changes due to the changing phases of the Moon; the signal is greatest when the Moon is full and decreases on either side of full. Figure 6 shows the signal change as a function of illumination of the Moon. The range of output voltages from the system can range between ±10VDC with the maximum value on the Full Moon near zenith at 18-19VDC. Figure 6 shows a decrease of ∼10VDC over a 3 day period. This rapid drop in signal sets a limit on the observation window. MooSci is used monthly over the period spanning ±6 days around the Full Moon. During the course of a night the signal also changes due to the changing altitude of the Moon. The signal change due to change in altitude is significantly smaller than that associated with the phases and is typically on the order of tenths of a volt.

The first MooSci began operations in June 2010. Both MooSci units achieve a S/N of 10^5 when the Moon is full and transiting and a S/N of $2.8\text{x}10^4$ when the Moon is low and out of phase (Villanueva et al. 2010). These values are calculated using MooSci's measured 100Hz noise of 0.18mV.

To further test the error in the measurements, MooSci was used as two separate 6 channel arrays. This configuration is equivalent to two side-by-side LuSci arrays with respect to detector spacing. The covariances between each detector were then obtained along with the difference in the covariances between each identical spacing between the two arrays. A histogram of these differences was made and is shown in Figure 7. The mean and variance of the entire data set was calculated and a gaussian plotted over the histogram. This is not a fit to the binned data presented in the histogram but is the full data. The mean of the full data set is $2.6095\text{x}10^{-10}$ and the standard deviation is $3.6319\text{x}10^{-9}$. The standard deviation reflects using data over the full atmospheric range of MooSci and shows greater differences at higher layers where the scintillation of extended objects is weaker.

MooSci meets it's operational requirements by detecting changes in the received signal with a S/N on the order of 10^4 or greater while operating with very low noise even at the higher atmospheric layers.

4.2. Lab Testing

Each photodiode module was tested in the laboratory before shipment of the instruments. It is crucial that no phase shift exist between the data collected by any pair of detectors. A phase shift in the detection would make a truly correlated signal appear to be uncorrelated. Since MooSci

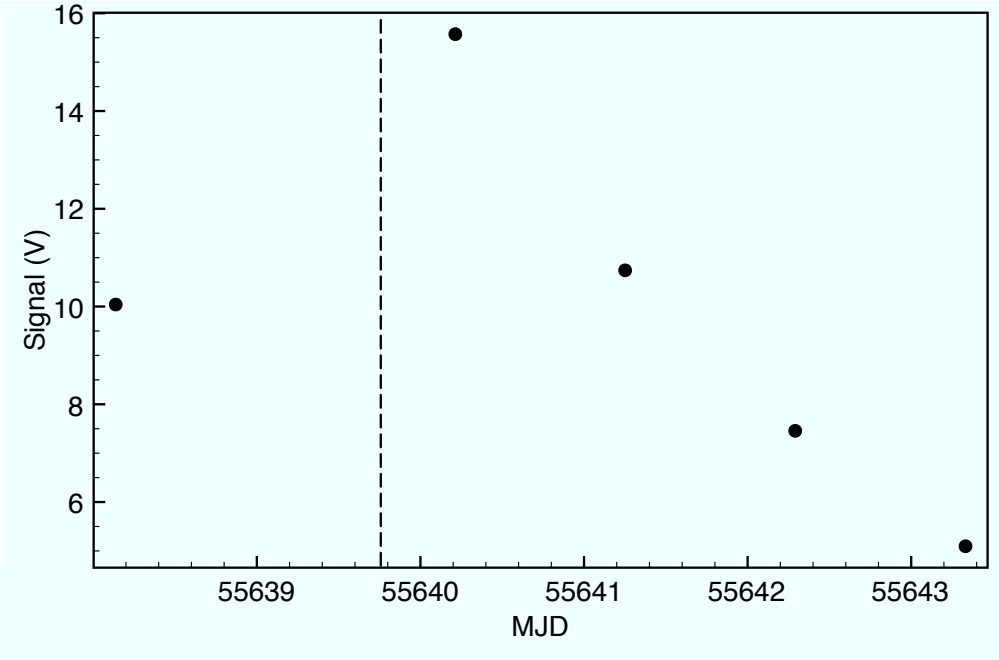

Fig. 6.— Signal vs time plot for MooSci. The MJD 55639 corresponds to 12am March 19$^{\text{th}}$ 2011. The dashed line is the time of the Full Moon for reference. Moon phase dramatically changes the signal received resulting in a change of $\sim$10V over a 3 day period outside of Full (MJD 55640-55643).

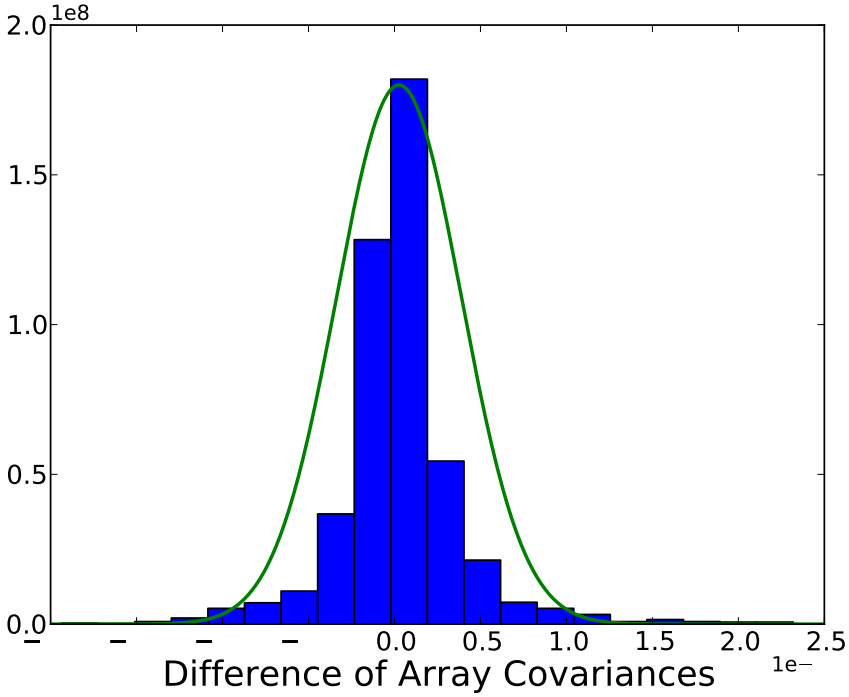

Fig. 7.— Histogram of the difference between like spacings when MooSci is used as two separate arrays. The data was collected over the night of 2010-09-23 when the Moon was at Full. The histogram is not a fit to the histogram but is plotted using the mean and variance of the full, unbinned data set.

operates by measuring covariances, the instrument must be able to accurately measure correlated signals. To ensure that there is no phase shift, each detector was exposed to a light emitting diode (LED) driven by a square wave. An oscilloscope was used on each channel to check the detected phase and make sure that it matched all the other channels as well as the phase produced by the function generator driving the LED. In the final design no phase shifts were detected.

Tests were also conducted that looked for signs of crosstalk in the channels. In these tests all the detectors were capped off but one. All detectors were exposed to a signal that matched that expected from the Moon and all channels were checked for response from the detectors. In the absence of crosstalk, only the uncovered channel should respond. This test was repeated for each detector in the array. In each test only the uncapped detector registered any signal; no signal increase was seen in the other detectors. In addition the running power spectrum in the software was used to identify any abnormalities in the signal including a 60Hz peak indicative of contamination from the power supply. No abnormal signals were detected.

5. Results

Complete instrument tests were conducted at the GMT site at LCO by members of the Giant Magellan Telescope Organization (Berdja et al. 2011). MooSci proved itself to be a reliable and easy-to-use instrument capable of obtaining quality covariance data.

Each MooSci unit has the ability to perform a self check. As discussed above, the array is symmetric about the center detector. With this arrangement it is possible to treat the instrument as two separate lunar scintillometers and compare the results of both. Since both arrays are at the same location, their results should be in good agreement. Figure 8 presents the results of such a test performed at Las Campanas Observatory using the original MooSci unit. MooSci1 refers to the covariances calculated from baselines formed from detectors 1-6 and MooSci2 to the covariances calculated from detectors 6-11. The points are for each baseline. A linear relationship with a slope of 1 emerges. Figure 7 was made using the covariance data presented here. A greater dispersion at larger detector spacings is seen as has been discussed previously. The precision of the average seeing calculated from the two arrays is better than 1%.

LuSci is a completed instrument that has been used in previous site characterization campaigns (Dali Ali et al. 2007). To further demonstrate that MooSci provides accurate data, it was co-located with a LuSci unit and the seeing calculated from both sets of data. The results of this test can be seen in Figure 9. The LuSci - MooSci difference between the nearest time stamps are also shown. It is important to note that only one LuSci sky measurement was available for the reduction process. Instead polynomial fits of the MooSci sky data from the same night were applied to the LuSci sky data. The results are shown while detailed discussion is deferred to Thomas-Osip et al. (2011). The two instruments confirm each other's measurements. Minor differences may be expected due to the difference in low frequency filtering between the two instruments and differences in the handling of

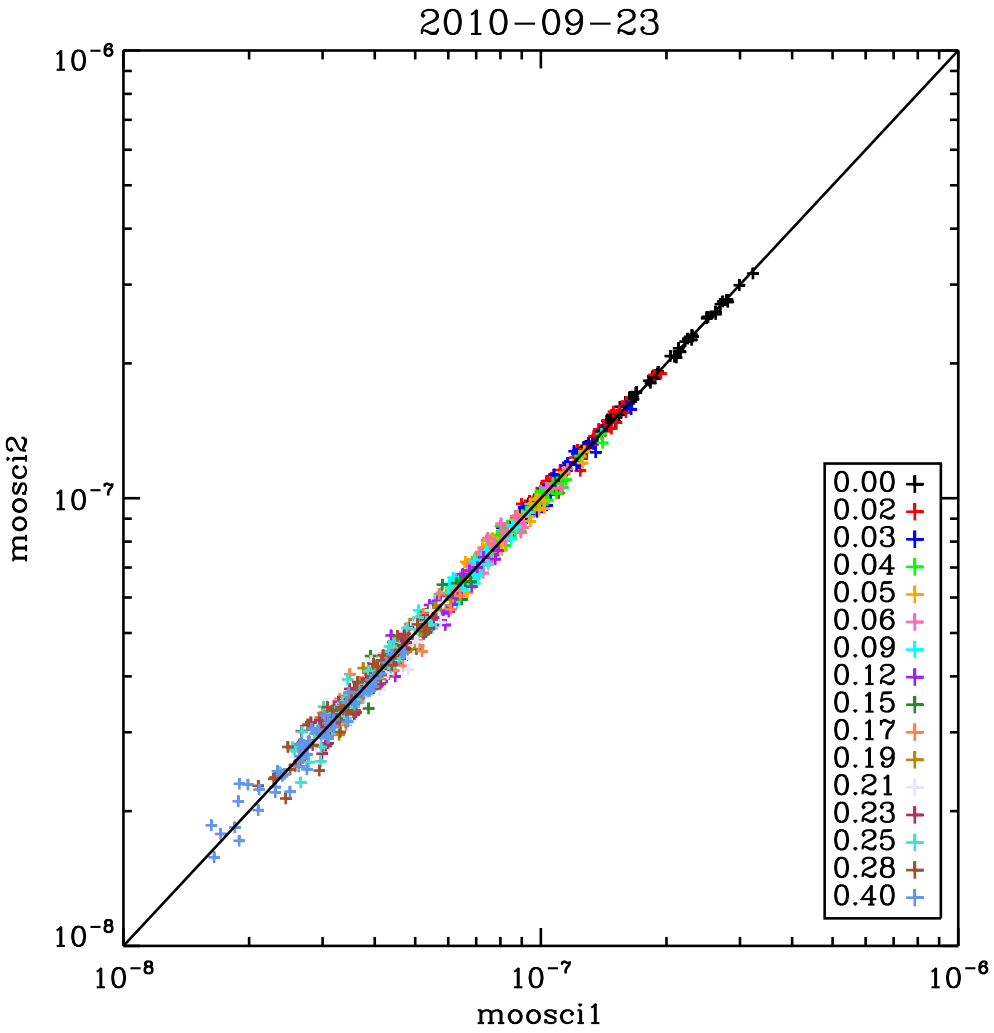

Fig. 8.— MooSci data taken with the instrument used as two separate arrays on September 23$^{\rm rd}$ 2010 (MJD 55462). The different colors show the different baselines possible using only one-half of the detectors. These baselines correspond to the LuSci baseline. The x- and y-axes give the measured covariance for the corresponding array.

the sky subraction. While MooSci is not fully automatic, it has proven to be simpler to operate than LuSci.

The second MooSci unit, MooTwo, was commissioned and providing data the same day that it arrived on site. With two units it is possible to place them side by side and ensure that there is good agreement between the two sets of instruments. This test was also conducted on site at Las Campanas Observatory upon delivery of MooTwo. The results are shown in Figure 10. Besides the tight correlation between the two instruments this also helped verify that the MooSci design can be reliably replicated. The full campaign is discussed by Berdja et al. (2011) and Thomas-Osip et al. (2011).

6. Conclusions

We have developed a new lunar scintillometer, MooSci, with a 0.8m long baseline that provides a ground layer atmospheric probe that can separate distinct atmospheric layers. MooSci features electronics with low optical and electronic crosstalk and signal processing that requires no low frequency data be removed. MooSci combines electronics capable of achieving a high S/N with a simple mechanical design and an easy-to-use user interface. Each MooSci unit is designed to provide an easy internal consistency test and multiple units allow further testing of unit-to-unit agreement. These tests, as they have been performed on MooSci and MooTwo, show that the MooSci design produces units capable of achieving high signal-to-noise while collecting data that allows for the reconstruction of atmospheric turbulence. These two units were used in the GMT site characterization campaign; discussed by Thomas-Osip et al. (2011).

We gratefully acknowledge Charles R. and Judith G. Munnerlyn for their support of the astronomical instrumentation lab at Texas A&M University, and George P. And Cynthia Woods Mitchell for their support of Physics and Astronomy at Texas A&M University. We further thank the staff of Las Campanas Observatory for their assistance while on site in Chile. We also thank Patrick Williams for his work in preparing Figure 5. This material is based in part upon supported AURA through the National Science Foundation under Scientific Program Order no. 10 as issued for support of the Giant Segmented Mirror Telescope for the United States Astronomical Community, in accordance with Proposal No. AST-0443999 submitted by AURA.

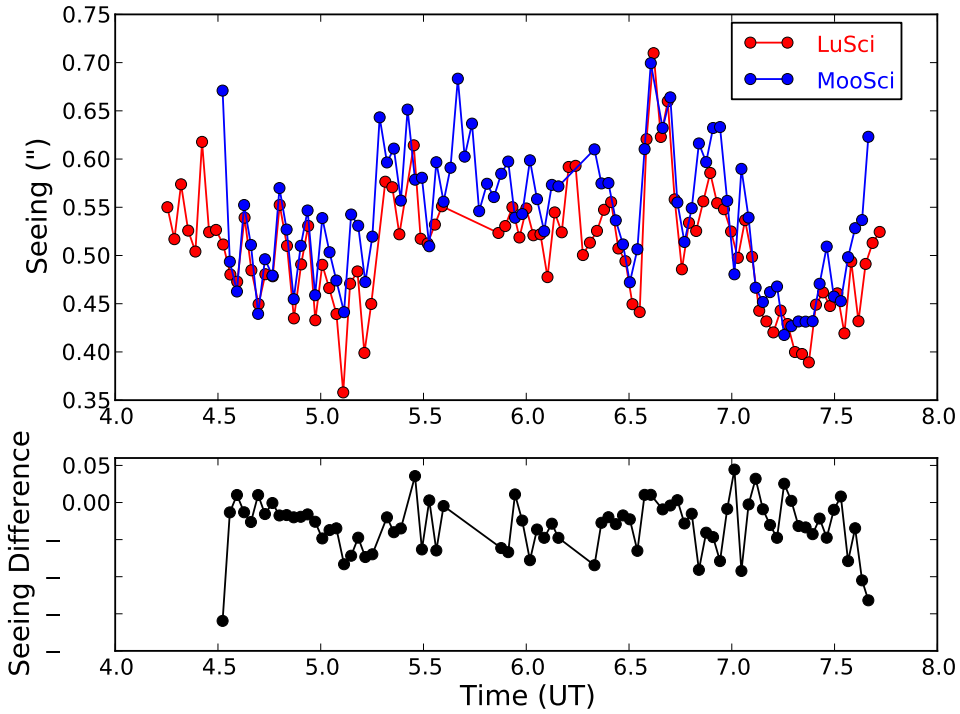

Fig. 9.— Plot of seeing vs time for MooSci and LuSci and the differences between the nearest time intervals. Differences are LuSci - MooSci. The agreement between the two instruments demonstrates MooSci's capability for measuring the ground layer turbulence of a site.

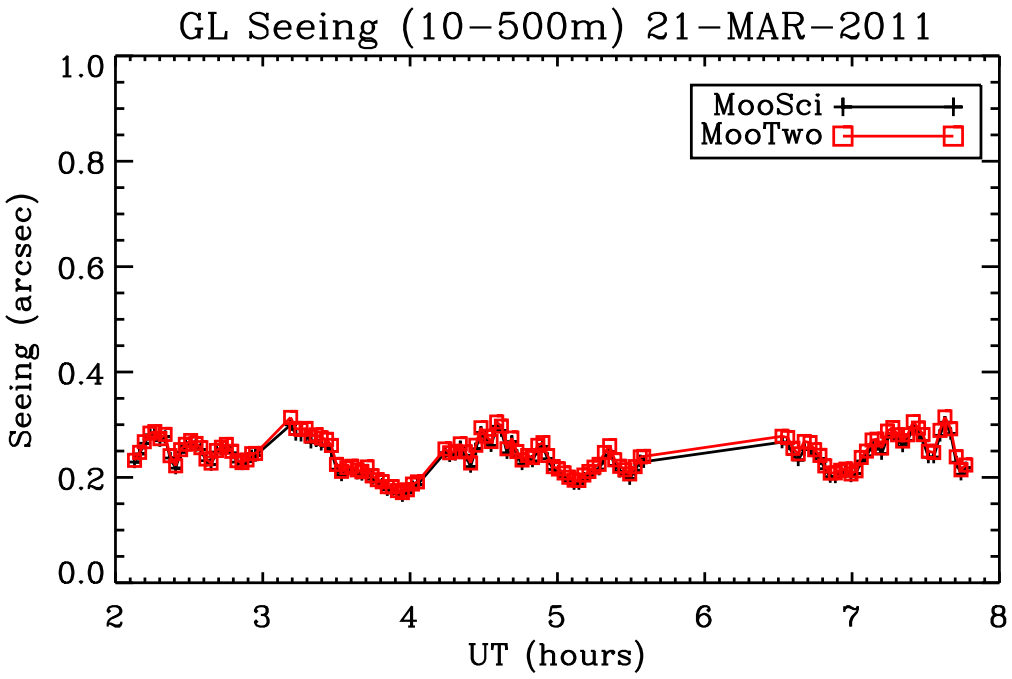

Fig. 10.— Plot of seeing vs time for MooSci and MooTwo while co-located at Las Campanas Observatory. The agreement confirms that the MooSci design can be reliably replicated.

REFERENCES

Beckers, J.M., Leon, E., Mason, J., & Wilkins, L. 2007, Sol. Phys. 176, 23-36

Berdja, A., Prieto, G., & Thomas-Osip, J.E. 2011, MNRAS, 416, 553-558

Dali Ali, W., Ziad, A., Berdja, A., Maire, J., Borgnino, J., Sarazin, M., Lombardi, G., Navarrete, J., Vazquez Ramio, H., Reyes, M., Delgado, J.M., Fuensalida, J.J., Tokovinin, A., & Bustos E. 2010, A&A, 524, A73+

Hickson, P. & Lanzetta, K., 2004, PASP, 116, 1143-1152

Rajagopal, J., Tokovinin, A., Bustos, E., & Sebag J. 2008, Proc. SPIE, 7013, 70131P, doi:10.1117/12.789042

Roddier, F. 1981, Prog. Opt., 19, 281

Thomas-Osip, J.E., Prieto, G., & Berdja, A. 2012, PASP, 124, 84-93

Tokovinin, A. 2007, Rev. Mex. AA, 31, 61-70

Tokovinin, A., Bustos, E., Berdja, A. 2010, MNRAS, 404, 1186-1196

Vernin, J., & Muñoz-Tuñón C. 1992, Astron. Astrophys. 257, 811-816

Villanueva Jr., S., DePoy, D.L., Marshall, J., Berdja, A., Rheault, J.P., Prieto, G., Allen, R., Carona, D. 2010, Proc. SPIE, 7735, 773547, doi:10.1117/12.857413